

Accepted Manuscript

Cloning and molecular characterization of two ferritins from red abalone *Haliotis rufescens* and their expressions in response to bacterial challenge at juvenile and adult life stages

Teodoro Coba de la Peña, Claudia B. Cárcamo, María I. Díaz, Federico M. Winkler, Byron Morales-Lange, Luis Mercado, Katherina B. Brokordt

PII: S1050-4648(18)30505-9

DOI: [10.1016/j.fsi.2018.08.030](https://doi.org/10.1016/j.fsi.2018.08.030)

Reference: YFSIM 5488

To appear in: *Fish and Shellfish Immunology*

Received Date: 17 April 2018

Revised Date: 8 August 2018

Accepted Date: 14 August 2018

Please cite this article as: Coba de la Peña T, Cárcamo CB, Díaz Maril, Winkler FM, Morales-Lange B, Mercado L, Brokordt KB, Cloning and molecular characterization of two ferritins from red abalone *Haliotis rufescens* and their expressions in response to bacterial challenge at juvenile and adult life stages, *Fish and Shellfish Immunology* (2018), doi: 10.1016/j.fsi.2018.08.030.

This is a PDF file of an unedited manuscript that has been accepted for publication. As a service to our customers we are providing this early version of the manuscript. The manuscript will undergo copyediting, typesetting, and review of the resulting proof before it is published in its final form. Please note that during the production process errors may be discovered which could affect the content, and all legal disclaimers that apply to the journal pertain.



1 **Cloning and molecular characterization of two ferritins from red**
2 **abalone *Haliotis rufescens* and their expressions in response to**
3 **bacterial challenge at juvenile and adult life stages**

4 Teodoro Coba de la Peña^{a#}, Claudia B. Cárcamo^{a,b#}, María I. Díaz^{a,c}, Federico M.
5 Winkler^{a,b,d}, Byron Morales-Lange^e, Luis Mercado^e, Katherina B. Brokordt^{a,b*}

6

7 ^a*Laboratorio de Fisiología y Genética Marina (FIGEMA), Centro de Estudios*
8 *Avanzados en Zonas Áridas (CEAZA) and Universidad Católica del Norte, Larrondo*
9 *1281, Coquimbo, Chile.*

10 ^b*Centro de Innovación Acuícola AquaPacífico, Facultad de Ciencias del Mar,*
11 *Universidad Católica del Norte, Larrondo 1281, Coquimbo, Chile.*

12 ^c*Programa de Magíster en Ciencias del Mar mención Recursos Costeros, Facultad de*
13 *Ciencias del Mar, Universidad Católica del Norte, Larrondo 1281, Coquimbo, Chile.*

14 ^d*Departamento de Biología Marina, Facultad de Ciencias del Mar, Universidad*
15 *Católica del Norte, Larrondo 1281, Coquimbo, Chile.*

16 ^e*Laboratorio de Genética e Inmunología Molecular, Instituto de Biología, Pontificia*
17 *Universidad Católica de Valparaíso, 2373223 Valparaíso, Chile*

18

19 # These authors contributed equally to the study

20 * Corresponding author: Katherina Brokordt,
21 katherina.brokordt@ceaza.cl / kbrokord@ucn.cl

22

23 **Abstract**

24 Ferritins are ubiquitous proteins with a pivotal role in iron storage and homeostasis, and
25 in host defense responses during infection by pathogens in several organisms, including
26 mollusks. In this study, we characterized two ferritin homologues in the red abalone
27 *Haliotis rufescens*, a species of economic importance for Chile, USA and Mexico. Two
28 ferritin subunits (*Hrfer1* and *Hrfer2*) were cloned. *Hrfer1* cDNA is an 807 bp clone
29 containing a 516 bp open reading frame (ORF) that corresponds to a novel ferritin
30 subunit in *H. rufescens*. *Hrfer2* cDNA is an 868 bp clone containing a 516 bp ORF that
31 corresponds to a previous reported ferritin subunit, but in this study 5'- and 3'-UTR
32 sequences were additionally found. We detected a putative Iron Responsive Element
33 (IRE) in the 5'-UTR sequence, suggesting a posttranscriptional regulation of *Hrfer2*
34 translation by iron. The deduced protein sequences of both cDNAs possessed the motifs
35 and domains required in functional ferritin subunits. Expression patterns of both
36 ferritins in different tissues, during different developmental stages, and in response to
37 bacterial (*Vibrio splendidus*) exposure were examined. Both *Hrfer1* and *Hrfer2* are most
38 expressed in digestive gland and gonad. *Hrfer1* mRNA levels increased about 34-fold
39 along with larval developmental process, attaining the highest level in the creeping post-
40 larvae. Exogenous feeding is initiated at the creeping larva stage; thus, the increase of
41 *Hrfer1* may suggest an immunity-related role upon exposure to bacteria. Highest
42 *Hrfer2* expression levels were detected at trochophore stage; which may be related with
43 early shell formation. Upon challenge with the bacteria an early mild induction of
44 *Hrfer2* (2 h post-challenge), followed by a stronger induction of *Hrfer1* at 15 h post-
45 challenge, was observed in haemocytes from adult abalones. While maximal
46 upregulation of both genes in the whole individual occurred at 24 h post-challenge, in
47 juveniles. A significant increase in ferritin protein levels from 6 h to 24 h post-challenge
48 was also detected. Our results suggest an involvement of *Hrfer1* and *Hrfer2*, and of
49 ferritin proteins in the immune response of *H. rufescens* to bacterial infection.

50

51 **Key words:** Ferritin; *Haliotis rufescens*; abalone immunity; *Hrfer1*; *Hrfer2*

52

53

54 1. Introduction

55 Ferritins are ubiquitous proteins that play a crucial role in iron storage and homeostasis,
56 regulating intracellular iron concentration and avoiding iron-induced oxidative damage
57 [1,2]. Typical vertebrate ferritins are multimeric proteins composed of 24 subunits
58 forming a nanocage structure with a capacity for storing up to 4500 atoms of iron in its
59 central cavity [2]. Each subunit is a protein chain folded in 4-helical bundles, a fifth
60 short helix and a long-extended loop [3]. In mammals, there are primarily two cytosolic
61 ferritin subtypes, the heavy (H) and light (L) chain types. H- and L-subunits can
62 assemble in different ratios to form the nanocage. The H chain has iron binding sites
63 with ferroxidase activity, oxidizing and actively sequestering iron. The L chain lacks
64 ferroxidase activity, but contains the ferrihydrite nucleation center, that is, several
65 negative charged residues in the inner surface that facilitate the transfer of oxidized iron
66 from the ferroxidase center to the iron core of the nanocage, iron hydrolysis,
67 mineralization and storage [4]. An additional ferritin middle (M) chain was
68 characterized in amphibians and bony fishes; M chain exhibits both, ferroxidase activity
69 and the ferrihydrite nucleation site [5,6]. Regarding their subcellular location in animals,
70 ferritins can be cytosolic, mitochondrial or secreted [2]. A post-transcriptional
71 regulation mechanism of ferritin expression in animals is mediated by the Iron
72 Regulatory Element (IRE), a regulatory sequence located at the 5' untranslated region
73 (5'-UTR) of ferritin mRNA. IRE forms a hairpin structure for binding to regulatory
74 proteins, which regulate translation of ferritin mRNAs depending on intracellular iron
75 concentrations [7,8].

76 Up to date, ferritin genes and functions were poorly studied in marine invertebrates
77 compared to vertebrates. In mollusks, H-type cytosolic and secretory ferritins have been
78 identified [9-14]. It was postulated that mollusk ferritins were involved in different
79 functional roles besides iron storage and release, as growth [15,16], shell development
80 [9,13,17], heavy metal detoxification [11], tolerance to thermal stress [18] and innate
81 immunity [10-12,14,16].

82 Abalone species of the genus *Haliotis* have a wide geographical distribution, and
83 several species are very important in fisheries and aquaculture industries because of
84 their high commercial value as food and jewelry, being cultured worldwide [19,20].
85 Global abalone production from legal fisheries has decreased over the last decades, due

86 to over-exploitation, disease and habitat degradation, promoting an important increase
87 in farm production in several countries [21]. The culture of red abalone (*Haliotis*
88 *rufescens*) was introduced in Chile in 1977, being currently this Country one of the
89 greatest producers of cultured abalone in the world [22,23]. However, natural and
90 cultured *Haliotis* spp. and other mollusks can suffer massive mortalities at larval, post-
91 larval and juvenile stages due to vibriosis, a deadly hemorrhagic septicemic disease
92 caused by pathogenic bacteria *Vibrio* spp. [24-27]. Thus, a better characterization of the
93 mechanisms of defense of red abalone to *Vibrio* spp. infections is necessary for the
94 development of strategies to control diseases and the development of its sustainable
95 farming.

96 The aim of the present study was to characterize *H. rufescens* ferritin genes and their
97 expression patterns related with early development and immune response. Here we
98 report the identification and characterization of two ferritin homologues cloned from *H.*
99 *rufescens*, designated as *Hrfer1* and *Hrfer2*. Ferritin cDNA sequences were analyzed
100 and gene transcriptional patterns were studied in different tissues, along larval
101 development and in juvenile and adult abalones challenged with *Vibrio splendidus*. In
102 order to analyze ferritin expression patterns during the bacterial challenge we further
103 produced and validated an anti-ferritin polyclonal antibody for *H. rufescens*.

104

105 **2. Materials and methods**

106 *2.1. Animals, bacterial challenge and sample collection*

107 Red abalone (*Haliotis rufescens*) individuals were grown at the abalone production
108 center (AWABI), Universidad Católica del Norte (Coquimbo, Chile). They were
109 maintained in a 1000 L raceway with flow-through seawater (mean temperature of
110 16°C) and fed *ad libitum* with *Macrocystis pyrifera* twice a week. Healthy adult
111 individuals (2 years old, shell length-ranged between 5 and 6 cm) were collected and
112 samples of several tissues (mantle, adductor muscle, gonads, gills and digestive tract)
113 were extracted and fixed in RNAlater Stabilization Reagent (Ambion Inc., Austin,
114 Texas, USA) and stored at -80°C.

115 Larvae at different stages of development were also collected. Adult red abalone
116 individuals were induced to spawn [28] and gametes were mixed together at

117 concentrations sufficient to allow for fertilization. Samples of gastrulae, trochophores,
118 veligers and creeping larvae were respectively collected at 6 h, 24 h, 3 days and 6 days
119 after fertilization; fixed in RNAlater and stored at -80°C for subsequent RNA
120 purification.

121 Challenge experiments were performed with the marine bacterial strain *Vibrio*
122 *splendidus*. *V. splendidus* was heat-attenuated in order to expose the abalones to a
123 pathogen associated molecular pattern (PAMP) immune stimulus and eliminate the
124 virulent component of the bacteria that could inhibit the immune response activation.
125 Bacteria were inactivated by heating and pellet was obtained as described in Coba de la
126 Peña et al. [16]. Pellet was then resuspended in sterile sea water at a final concentration
127 of 1×10^7 cells/mL. Forty-four adult or juvenile (12 mo. old, shell length of 1.0-1.5 cm)
128 abalones were randomly divided into three groups. One group consisted on 20
129 individuals that were challenged by injection of 100 μ L of the *V. splendidus* suspension
130 in sterile seawater (1×10^7 cells/mL) in the adductor muscle using a 25 G syringe. The
131 second group consisted on 20 individuals that were injected with 100 μ L of sterile
132 seawater and were used as controls. One mL of hemolymph from 4 individuals in each
133 group was collected after 2, 6, 15 and 24 h of injection at the adult stage. An additional
134 control group (basal status) of four individuals not subjected to injection was assessed,
135 and from which haemolymph was collected at time 0 h. Collected haemolymph samples
136 were immediately centrifuged at 600 g at 4°C for 10 min to harvest the haemocytes.
137 Haemocytes were then immediately fixed in RNAlater and stored at -80°C. In juvenile
138 abalones was not possible to collect enough haemolymph, thus whole individuals from
139 each group were sampled after 6, 15, 24 and 48 h post injection. Their tissues were deep
140 frozen and pulverized with liquid nitrogen and stored at -80°C for the analyses of
141 ferritin mRNA and protein levels.

142 Animal maintenance and handling were carried out in strict accordance with the
143 recommendations in the CCAC guidelines
144 (<http://www.ccac.ca/Documents/Standards/Guidelines>).

145 2.2. RNA extraction, first strand cDNA synthesis and isolation of *Hrfer1* and *Hrfer2* 146 full-length cDNAs

147 Total RNA extraction, RNA quantification and intactness, and reverse transcription of
148 RNAs from samples were performed as described in Coba de la Peña et al. [16].

149 In order to isolate at least two different *H. rufescens* ferritin homologues, two different
150 pairs of oligonucleotides were used. The first primer pair, 5'-
151 CCCACAAAGCACGTAACGAA-3' (forward) and 5'-
152 CACGCCATACTGTTATAGGG-3' (reverse), were designed from conserved ferritin
153 sequences that are available at the NCBI GenBank Sequence Database
154 (<http://www.ncbi.nlm.nih.gov/genbank>) using the Primer3web program v4.0.0
155 (<http://bioinfo.ut.ee/primer3/>). A 485-bp PCR product from mantle cDNA of adult
156 individuals was amplified, purified and sequenced by Servicio de Secuenciación de la
157 Pontificia Universidad Católica de Chile. In order to isolate the full coding DNA
158 sequence of the *H. rufescens* ferritin homologue, RACE (Rapid Amplification of cDNA
159 ends) was performed using the SMARTerTM RACE cDNA Amplification Kit (Clontech,
160 Palo Alto, CA, USA). Approximately 1 µg of RNA from *H. rufescens* mantle was used
161 for first-strand DNA synthesis, obtaining 5'-RACE-Ready cDNA and 3'-RACE-Ready
162 cDNA. Specific primers for 5'- and 3'-RACE PCR were designed to recognize a region
163 within the cDNA previously isolated and sequenced. Primer sequences were: 5'-
164 GTCAGTGTTGCAGTCCGCCACCTTG TG-3' (5'-RACE) and 5'-
165 GGCGGGCGTCAACAAACAGATTAACGT-3' (3'-RACE). Thermal cycling
166 parameters were set following manufacturer's instructions. The amplification products
167 were visualized, cloned, sequenced and aligned as described in Coba de la Peña et al.
168 [16].

169 In order to obtain a second *H. rufescens* ferritin homologue, a second primer pair was
170 designed based in a published *H. rufescens* ferritin coding sequence (GenBank
171 accession number GU191936; [18]). Primers were: 5'-GATGGCCCAAACCTCAACC-3'
172 (forward) and 5'-GGTTATGTCAGCCCAAACAAA-3' (reverse). PCR performed with
173 these primers generated a 700-bp PCR product that was cloned and sequenced. In order
174 to obtain the 5' untranslated region (5-UTR), 5'-RACE PCR was performed using 5'-
175 RACE-ready cDNA and a specific primer designed to recognize a sequence within the
176 700-bp cDNA previously isolated and sequenced. Primer sequence was 5'-
177 TCAGCTTCTCGGCATGCTCTCGCTCCT-3'. The obtained PCR product was cloned,
178 sequenced and aligned.

179 *2.4. Sequence analyses*

180 Sequences were analyzed by BLAST algorithm at the National Center for
181 Biotechnology Information. Nucleotide sequences were translated to predicted protein
182 sequences and aligned with known ferritin sequences using the Expasy web server tools
183 (<http://www.expasy.org/>). The iron responsive element (IRE) and stem-loop structure of
184 *Hrfer2* was predicted by the SIREs Web Server v2.0 (<http://ccbg.imppc.org/sires/>) [29].
185 The tertiary structures of deduced proteins codified by *Hrfer1* and *Hrfer2* were
186 predicted using the Phyre² server [30]. Phylogenetic analysis was performed with
187 MEGA (Molecular Evolutionary Genetic Analysis) software v6.06 [31] using the
188 neighbour-joining method [32], with bootstrap values calculated from 2,000 pseudo-
189 replicates.

190 2.5. Quantitative real-time PCR

191 Primers for RT-qPCR were designed using Primer Express v3.0 software (Applied
192 Biosystems, CA, USA). The amplified region included a partial 3'-UTR sequence, in
193 order to amplify specifically the gene homologs under study. β -actin was used as
194 endogenous control in order to normalize experimental results [18,33]. Primer
195 sequences were as follows: *Hrfer1* (forward, 5'-CAGGTCTCGGAGAGTACCAGTTC-
196 3'; reverse, 5'-GGCCGCGGACCAATTAAC-3'); *Hrfer2* (forward, 5'-
197 ACGACAAGGAGTCCATGGAGTAG-3'; reverse, 5'-GGCCACGTGCGACTATGC-
198 3'); β -actin (forward, 5'-GAGAGGTTCCGTTGTCCAGAGT-3'; reverse, 5'-
199 CCAGCAGATTCCATACCCAAGA-3').

200 RT-qPCR assays were run as described in Coba de la Peña et al. [16]. The comparative
201 C_T method [34] was applied for relative quantification. Experiments included five
202 biological replicates except in larvae expression (three biological replicates), and three
203 technical replicates were performed.

204 2.6. Production and validation of anti-ferritin polyclonal antibody, ELISA and Western 205 Blotting

206 Polyclonal antibodies were generated in CF-1 mice (6 weeks old) against a mix of three
207 synthetic antigenic epitopes of ferritin from *H. rufescens* (UniProtKB - Q0PKG1) (Fig.
208 S1). These epitopes were designed using a method described by Bethke et al. [35] and
209 they were chemically synthesized by the solid phase multiple peptide system using
210 Fmoc amino acids (Iris Biotech); and purified through HPLC. The peptides were

211 lyophilized and analyzed by matrix assisted laser desorption/ionization mass
212 spectrometry to confirm molecular mass [36]. For antibody production, CF1 mice were
213 subcutaneously injected at 1, 14 and 28 days with 300 µg of ferritin peptide mix (100 µg
214 each one) diluted 1:1 in FIS peptide (peptide sequence: FISEAIIHVLHSR), a T helper
215 cell activator [37], and 1:1 in Freund's adjuvant (Thermo). The antiserum was collected
216 on day 44, centrifuged at 800 x g for 10 min and the supernatant was stored at -20 °C.
217 Antibody affinity was determined by indirect ELISA [38] and antibody specificity was
218 verified by Western blot using a total protein extract of *H. rufescens* following Schmitt
219 et al. [39] (Fig. S1). Indirect ELISA was used to quantify the ferritin expression in the
220 juveniles from the challenge experiment following Morales-Lange et al. [38], but using
221 1:2500 ferritin antisera.

222 2.6. Statistical analyses

223 Data were analysed with the STATISTICA v7.0 software package (StatSoft Inc., Tulsa,
224 OK, USA). The following statistical tests were performed: one-way analysis of variance
225 (one-way ANOVA) and Tukey post-hoc test for data of gene expression in tissues and
226 larvae. Data of gene expression upon bacterial challenge were analysed by factorial
227 ANOVA (in order to assess the effect of two factors: presence or absence of bacteria
228 and time post-challenge) and Tukey post-hoc test. We applied a sequential Bonferroni
229 procedure to correct for type I error in multiple simultaneous tests. Differences were
230 considered significant at $P < 0.05$. For ANOVAs, normality of the dependent variable
231 was tested with the Shapiro-Wilks test [40] and homogeneity of variances with the
232 Levene test [41] to verify that the data met model assumptions.

233

234 3. Results and discussion

235 3.1. cDNA cloning and sequence characterization of *Hrfer1* and *Hrfer2*

236 Two full-length cDNA clones were isolated from mantle of *H. rufescens*, and they were
237 designated as *Hrfer1* (for *H. rufescens* ferritin 1, GenBank accession no. MH006611)
238 and *Hrfer2* (GenBank accession no. MH006612). They were 807 and 868 bp length,
239 respectively. The open reading frames (ORFs) of *Hrfer1* and *Hrfer2* are 516 bp length,
240 encoding 171 amino acids. Molecular weights of *Hrfer1* and *Hrfer2* predicted proteins
241 are 19.9 and 19.8 kDa, respectively. Predicted isoelectric points are 5.04 and 5.09,

242 respectively. By homology search, it was observed that *Hrfer2* coding sequence and
243 part of the 3'-UTR sequence corresponded to a ferritin gene (designed as *Abf2*)
244 previously identified in *H. rufescens* (Genbank accession number GU191936; [18]).
245 Seven conserved residues, corresponding to the ferroxidase diiron center, which
246 catalyzes Fe(II) oxidation in mammalian H ferritins, were identified in both *Hrfer1*
247 (L25, Y32, K59, K60, F63, E105, E139) (Fig. 1A) and *Hrfer2* ([18]; Fig. 1B) predicted
248 proteins. Four conserved amino acids corresponding to the ferrihydrite nucleation center
249 of mammalian L-type ferritin subunits were observed in both *Hrfer1* (D55, C58, K59,
250 E62) and *Hrfer2* (K55, E58, E59, E62) predicted proteins (Fig. 1A and 1B). Both
251 sequences also displayed conserved iron ion channel amino acids (H116, D129, E132)
252 (Fig. 1A and 1B). *Hrfer1* predicted protein has a putative N-glycosylation site
253 (27NCSY30). Thus, *Hrfer1* presented all sequence motifs determining ferritin function
254 [1,18,42]. As M-type ferritins, both genes have both the ferroxidase activity observed in
255 H-type ferritins and the ferrihydrite nucleation center observed in L-type ferritins [2].
256 No putative signal peptide was detected, which suggested that both predicted ferritins
257 are cytosolic proteins.

258 Multiple sequence alignment showed that *Hrfer1* and *Hrfer2* displayed high amino acid
259 identities with other mollusk, invertebrate and vertebrate ferritin homologues (Fig. S2).
260 *Hrfer1* corresponded to a new ferritin homologous sequence and showed 98% amino
261 acid identity with a ferritin of *Haliotis discus hannai* (GenBank accession no.
262 ADK60915). *Hrfer2* corresponded to a sequence previously described by Salinas-Clarot
263 et al. [18] with high amino acid homology with other *H. discus hannai* ferritin
264 homologue (GenBank accession no. ABH10672). *Hrfer1* showed 64% amino acid
265 identity with *Hrfer2*.

266 *Hrfer1* and *Hrfer2* 3D models consisted of four α helixes from the N-terminal that were
267 parallel with each other, binding together through random coils and turns (Fig. S3A and
268 S3B). A fifth short C-terminal α helix was also present in both proteins. Thus, predicted
269 3D models of *Hrfer1* and *Hrfer2* resembled the typical spatial features of known H- and
270 M-type ferritin protein structures [3,42].

271 Phylogenetic analysis of most known ferritin nucleotide coding sequences of mollusks
272 revealed that both *Hrfer1* and *Hrfer2* sequences are included into a clade of cytosolic,
273 non-secretory ferritins (Fig. S4). *Hrfer1*, with other *Haliotis* sequences, is into a cluster
274 that is separated from a big cluster containing all other non-secretory ferritins. *Hrfer2* is

275 into is included into a clade with other *Haliotis* sequences, and this clade further
276 clustered together with other *Argopecten*, *Mizuhopecten* and *Azumapecten* sequences in
277 the main (Fig. S4).

278 A putative iron responsive element (IRE) was identified by analysis of the 5'-UTR of
279 the *Hrfer2* cDNA clone. Alignment of the *Hrfer2* IRE sequence showed 100% identity
280 to known IREs of *H. discus discus*, *H. discus supertexta*, *H. discus hannai*, and other
281 mollusks (Fig. S5A). This IRE of *Hrfer2* is predicted to be folded in a typical stem-loop
282 secondary structure, which matches all IRE characteristics, (Fig. S5B). No IRE was
283 detected in the case of *Hrfer1*, probably because *Hrfer1* cDNA clone lacks whole 5'-
284 UTR sequence. The presence of this IRE suggests a posttranscriptional regulation of
285 *Hrfer2* translation [7,8].

286 3.2. Tissue-specific expressions of *Hrfer1* and *Hrfer2*

287 Transcriptional levels of both genes were detected in all tissues examined (Fig. 2).
288 Levels of mRNA of both genes were higher in digestive gland (36.9- and 35.5-fold
289 higher compared to muscle for *Hrfer1* and *Hrfer2*, respectively) and gonad (21.3- and
290 30.9-fold higher, respectively), and lowest level was observed in mantle, adductor
291 muscle and gill (Fig. 2A and 2B). Our results differed from those reported by Salinas-
292 Clarot et al. [18] for *Hrfer2* mRNA levels in the tissues. This could be associated to
293 differences in the age or general physiological status of the analyzed abalone in each
294 study.

295 Relative high basal levels of *ferritin* transcripts in digestive gland were also observed in
296 other mollusks, as *Crassostrea gigas* [43], *Argopecten purpuratus* [16], *H. discus discus*
297 [44], *H. diversicolor supertexta* [45] and *H. diversicolor* [46]. In abalone and other
298 mollusks, the digestive gland is involved in iron storage, metal accumulation and
299 detoxification [47,48]. Digestive gland is also an important immune organ involved in
300 defense functions and in the integration of metabolism and immunity [48,49]. Thus,
301 *Hrfer1* and *Hrfer2* may play an important role in iron storage and immune functions in
302 digestive glands.

303 Relative high basal levels of ferritin expression in gonad were also observed in *H.*
304 *discus discus* [44]. Abalone and mussels can uptake iron from the environmental
305 seawater, and this iron can be accumulated in several organs, including gonads [47,50].

306 It was also observed that expressions of two ferritin genes are induced in gonad of the
307 freshwater pearl mussel *Hyriopsis schlegelii* upon bacteria or heavy metal challenge
308 [51]. Thus, *Hrfer1* and *Hrfer2* expression in gonad may be related with iron
309 homeostasis and/or immune defense. Also, high levels of ferritin in gonads could be
310 associated to maternal transfer of immune proteins through the eggs (i.e., passive
311 immunity) to protect newly hatched larvae in abalone. This strategy has been observed
312 in other mollusks [52], but further studies would be necessary to elucidate if it is present
313 in abalone.

314 3.3. *Hrfer1* and *Hrfer2* expression in different developmental stages

315 Ferritin may be involved in mollusk shell formation during larval development
316 [9,13,17]. The first steps of the larval shell formation take place during the trochophore
317 stage [53]. In gastropods, ferritin genes are expressed in the edge of the shell field
318 during the trochophore stage [54,55]. A role of ferritin in construction of the operculum
319 was also suggested [54]. Transcriptional analysis of *Hrfer1* during larval development
320 of *H. rufescens* showed an increase of its level along the different developmental stages,
321 from gastrula (1-fold) to trochophore (about 4.3-fold higher than in gastrula), veliger
322 (18.4-fold) and creeping larva (33.8-fold) (Fig. 3A). A similar ferritin expression pattern
323 from eggs or gastrulae to juveniles was observed in the gastropod *H. asinine* [54] and
324 *Aplysia californica* [56]. *Hrfer1* expression pattern suggests that this ferritin homologue
325 may be involved in both protoconch (larval shell) and teleconch (juvenile/adult shell)
326 formation from trochophore to creeping larval stage, being the continuous increase in
327 expression from gastrulation to post-metamorphosis correlated with an increasing
328 demand in biomineralization. Other putative functional roles of *Hrfer1* cannot be
329 excluded. Development of the buccal apparatus in abalone post-larvae (creeping larva
330 stage) initiates exogenous feeding, which include bacteria [57]. Thus, the observed
331 significant increase of *Hrfer1* transcription level in abalone creeping larvae may suggest
332 and immunity-related role upon exposure to bacteria, as suggested for some ferritin
333 homologues characterized in different developmental stages of *C. gigas* [13] and *A.*
334 *purpuratus* [58].

335 In contrast, *Hrfer2* expression was higher in gastrula (1-fold) and in trochophore stage
336 (1.56-fold higher than in gastrula), and decreased in subsequent veliger (0.58-fold) and
337 creeping larva (0.26-fold) stages (Fig. 3B). *Hrfer2* may play a role as mitogen for cell

338 proliferation, as it was observed in animal models [59,60]. *Hrfer2* expression may also
339 be related with the first steps in larval shell formation at the trochophore stage [61].

340 3.4. Expression of *Hrfer1* and *Hrfer2* in response to bacterial challenge

341 In haemocytes from adult abalone *Hrfer1* expression was significantly up-regulated
342 after 15 h post-injection with *Vibrio splendidus* (4.5-fold compared to 1-8-fold of its
343 control injected with SSW or not injected), and declined afterwards (Fig. 4A). *Hrfer2*
344 was found to be slightly but significantly upregulated after 2 h, and a down-regulation
345 of *Hrfer2* was observed at 6 h post-injection with the bacteria (1.6-fold), compared with
346 its control (2.6-fold) (Fig. 4B). *Ferritin* transcriptional induction in response to bacterial
347 challenge was also observed in haemocytes of bivalve mollusks as *A. irradians* [10,62],
348 *A. purpuratus* [16] and *Hyriopsis schlegelii* [51], among others. Qiu et al. [63] observed
349 an upregulation of a *ferritin* homologue in haemocytes of *H. discus hannai* upon
350 infection with the bacterial pathogen *Vibrio anguillarum* in a time-dependent manner,
351 with a maximum expression level at 6 h post-inoculation. Our results suggest an
352 involvement of *Hrfer1* and *Hrfer2* in the immune response of *H. rufescens* to pathogen
353 infection. Ferritin upregulation upon bacterial infection may be related with the iron
354 withholding activity of ferritins, preventing host iron acquisition by bacteria [64]. A
355 putative antioxidant activity of ferritins, by preventing the generation of free radicals
356 and reactive oxygen species by iron, was also proposed [2].

357 In juvenile abalones, significant up-regulations of *Hrfer1* and *Hrfer2* levels were
358 observed after 24 h (respectively, 5.1 and 6.6-fold compared to 2.6 and 3.3-fold of their
359 control injected with sterile sea water) and 48 h (respectively, 3.4 and 2.7-fold
360 compared to 1.7 and 1.5-fold) post-injection with the bacterial suspension (Figs. 4C and
361 4D). *Ferritin* upregulation upon pathogen challenge was also observed in different
362 tissues of bivalves as *Mizuhopecten yessoensis* [11,14], and *Hyriopsis schlegelii* [51];
363 and of gastropods as *H. tuberculata* [65], *H. diversicolor* [46] and *H. discus hannai*
364 [63]. Thus, ferritin homologues may be induced upon pathogen inoculation in several
365 organs in different time-manners. Our results suggest that both *Hrfer1* and *Hrfer2* genes
366 are probably induced in one or several tissues (besides hemocytes) upon infection, and
367 maximum upregulation of both genes in the whole individual occurs at 24 h post-
368 injection.

369 3.5. Ferritin protein levels in response to bacterial challenge

370 Further investigation to detect and to estimate ferritin protein levels during bacterial
371 challenge was performed. The produced polyclonal antibody cannot discriminate
372 between ferritin isoforms of *H. rufescens*; thus considering the similar transcriptional
373 pattern observed for *Hrfer1* and *Hrfer2* in juveniles, ferritin protein levels were assessed
374 in extracts from whole individual at this stage. Significant higher amounts of ferritin
375 protein were detected in individuals challenged with bacteria at 6, 15 and 24 h post-
376 injection, compared with their respective controls injected with sterile seawater (or not
377 injected juveniles). No significant higher amount of protein was observed in challenged
378 individuals 48 h post-injection (Fig. 5).

379 We have identified two ferritin homologues in *H. rufescens*, but more ferritin
380 homologues may be expressed in this organism. For instance, two cytosolic and two
381 secretory ferritin homologues were identified in *C. gigas* [13], and four cytosolic and
382 two secretory ferritin homologues were identified in *Mizuhopecten yessoensis* [13,14].
383 Thus, our results suggest that there is a significant overexpression of ferritin protein
384 homologues (possibly including *Hrfer1*, *Hrfer2* and other ferritin homologues) in whole
385 individuals of *H. rufescens* from 6 to 24 h post-injection. This result suggests that,
386 besides *Hrfer1* and *Hrfer2*, other ferritin homologues are induced and involved in the
387 immune response to bacterial infection in *H. rufescens*.

388 In summary, our results showed that both ferritin homologues *Hrfer1* and *Hrfer2*
389 participate in the immune response against bacterial challenges in haemocytes and
390 probably in other tissue organs; and that the novel *Hrfer1* could be implicated in post-
391 larvae immunity. These results indicate that these ferritins are potential candidate genes
392 to be used as molecular markers for enhancement of immune capacity in *H. rufescens*
393 through genetic programmes. However, functional characterization experiments
394 involving the interference of expression of both genes and/or the expression of the
395 recombinant ferritin proteins will be necessary to verify the involvement of these genes
396 in *H. rufescens* immunity.

397

398 **Acknowledgements**

399 We gratefully acknowledge Dr. Rodrigo Rojas for bacteria procurement, and
400 technicians from the Abalone Culture Center (AWABI) for abalone maintenance.

401 Funding: This study was supported by National Fund of Science and Technology,
402 FONDECYT No 1140849 to K.B., F.W. and L.M.

403

404 **References**

- 405 [1] E.C. Theil, Ferritin: structure, gene regulation and cellular functions in animals,
406 plants and microorganisms. *Annu. Rev. Biochem.* 56 (1987) 289-315.
- 407 [2] P. Arosio, R. Ingrassia, P. Cavadini, Ferritins: a family of molecules for iron storage,
408 antioxidation and more. *Biochim. Biophys. Acta* 1790 (2009) 589-599.
- 409 [3] R.R. Crichton, J.P. Declercq, X-ray structures of ferritins and related proteins.
410 *Biochim. Biophys. Acta* 1800 (2010) 706-718.
- 411 [4] P. Arosio, S. Levi, Cytosolic and mitochondrial ferritins in the regulation of cellular
412 iron homeostasis and oxidative damage. *Biochim. Biophys. Acta* 1800 (2010) 783-
413 792.
- 414 [5] L.F. Dickey, S. Sreedharan, E.C. Theil, J.R. Didsbury, Y.H. Wang, R.E. Kaufman,
415 Differences in the regulation of messenger RNA for housekeeping and specialized-
416 cell ferritin. A comparison of three different ferritin complementary DNAs, the
417 corresponding subunits, and identification of the first processed in amphibia. *J.*
418 *Biol. Chem.* 262 (1987) 7901-7907.
- 419 [6] A. Giorgi, G. Mignogna, G. Bellapadrona, M. Gattoni, R. Chiaraluce, V. Consalvi,
420 E. Chiancone, S. Stefanini, The unusual co-assembly of H- and M-chains in the
421 ferritin molecule from the Antarctic teleosts *Trematomus bernachii* and *Trematomus*
422 *newnesi*. *Arch. Biochem. Biophys.* 478 (2008) 69-74.
- 423 [7] E.C. Theil, Iron regulatory elements (IREs): a family of mRNA non-coding
424 sequences. *Biochem. J.* 304 (1994) 1-11.
- 425 [8] E.C. Theil, IRE mRNA riboregulators use metabolic iron (Fe^{2+}) to control mRNA
426 activity and iron chemistry in animals. *Metallomics* 7 (2015)15-24.

- 427 [9] X. Wang, B. Liu, J. Xiang, Cloning, characterization and expression of ferritin
428 subunit from clam *Meretrix meretrix* in different larval stages. *Comp. Biochem.*
429 *Physiol. B* 154 (2009)12-16.
- 430 [10] X. He, Y. Zhang, X. Wu, S. Xiao, Z. Yu, Cloning and characterization of two
431 ferritin subunit genes from bay scallop, *Argopecten irradians* (Lamarck 1819). *Mol.*
432 *Biol. Rep.* 38 (2011) 2125-2132.
- 433 [11] L. Zhang, W. Sun, W. Cai, Z. Zhang, Y. Gu, H. Chen, S. Ma, X. Jia, Differential
434 response of two ferritin subunit genes (*VpFer1* and *VpFer2*) from *Venerupis*
435 *philippinarum* following pathogen and heavy metals challenge. *Fish Shellfish*
436 *Immunol.* 35 (2013a) 1658-1662.
- 437 [12] Y. Zhang, R. Zhang, J. Zou, X. Hu, S. Wang, L. Zhang, Z. Bao, Identification and
438 characterization of four ferritin subunits involved in immune defense of the Yesso
439 scallop (*Patinopecten yessoensis*). *Fish Shellfish Immunol.* 34 (2013b) 1178-1187.
- 440 [13] P. Huan, G. Liu, H. Wang, B. Liu, Multiple ferritin subunit genes of the Pacific
441 oyster *Crassostrea gigas* and their distinct expression patterns during early
442 development. *Gene* 546 (2014) 80-88.
- 443 [14] Y. Sun, Y. Zhang, X. Fu, R. Zhang, J. Zou, S. Wang, X. Hu, L. Zhang, Z. Bao,
444 Identification of two secreted ferritin subunits involved in immune defense of
445 Yesso scallop *Patinopecten yessoensis*. *Fish Shellfish Immunol.* 37 (2014) 53-59.
- 446 [15] Z. Bai, Y. Yuan, G. Yue, J. Li, Molecular cloning and copy number variation of a
447 ferritin subunit (*Fth1*) and its association with growth in freshwater pearl mussel
448 *Hyriopsis cumingii*. *PLoS ONE* 6 (2011) e22886.
- 449 [16] T. Coba de la Peña, C.B. Cárcamo, M.I. Díaz, K.B. Brokordt, F.M. Winkler,
450 Molecular characterization of two ferritins of the scallop *Argopecten purpuratus*
451 and gene expressions in association with early development, immune response and
452 growth rate. *Comp. Biochem. Physiol. B* 198 (2016) 46-56.
- 453 [17] I. Zhang, Q. Meng, T. Jiang, H. Wang, L. Xie, R. Zhang, A novel ferritin subunit
454 involved in shell formation from the pearl oyster (*Pinctada fucata*). *Comp.*
455 *Biochem. Physiol. B* 135 (2003) 43-54.

- 456 [18] K. Salinas-Clarot, A.P. Gutiérrez, G. Núñez-Acuña, G. Gallardo-Escárate,
457 Molecular characterization and gene expression of ferritin in red abalone (*Haliotis*
458 *rufescens*). *Fish Shellfish Immunol.* 30 (2011) 430-433.
- 459 [19] R. Gordon, P. Cook, World abalone fisheries and aqua-culture update: supply and
460 market dynamics. *J. Shellfish Res.* 23 (2004) 935–940.
- 461 [20] F. Lafarga de la Cruz, C. Gallardo-Escárate, Intraspecies and interspecies hybrids
462 in *Haliotis*: natural and experimental evidence and its impact on abalone
463 aquaculture. *Rev. Aquacult.* 3 (2011) 74-79.
- 464 [21] P.A. Cook, The worldwide abalone industry. *Modern Economy* 5 (2014) 1181-
465 1186.
- 466 [22] R.A. Flores-Aguilar, A. Gutiérrez, A. Ellwanger, S. Searcy-Bernal, Development
467 and current status of abalone aquaculture in Chile. *J. Shellfish Res.* 26 (2007) 705-
468 711.
- 469 [23] FAO. 2016. The State of World Fisheries and Aquaculture: Contributing for Food
470 Security and Nutrition for All. Food and Agriculture Organization of the United
471 Nations. FAO, Rome.
- 472 [24] R. Elston, G.S. Locwood, Pathogenesis of vibriosis in cultured juvenile red
473 abalone, *Haliotis rufescens* Swainson. *J. Fish. Dis.* 6 (1983) 111-128.
- 474 [25] C. Anguiano-Beltrán, R. Searcy-Bernal, M.L. Lizárraga-Partida, Pathogenic effects
475 of *Vibrio alginolyticus* on larvae and postlarvae of the red abalone *Haliotis*
476 *rufescens*. *Dis. Aquat. Org.* 33 (1998) 119-122.
- 477 [26] C. Rojas-Villalobos, Causas de mortalidad del abalón rojo (*Haliotis rufescens*) en
478 etapa de engorda en el período otoño-invierno (2005) PhD. Valdivia, Chile.
- 479 [27] J. Cai, Y. Han, Z. Wang, Isolation of *Vibrio parahaemolyticus* from abalone
480 (*Haliotis diversicolor supertexta* L.) postlarvae associated with mass mortalities.
481 *Aquaculture* 257 (2006) 161-166.
- 482 [28] D.E. Morse, H. Duncan, N. Hooker, A. Morse, Hydrogen peroxide induces
483 spawning in mollusks, with activation of prostaglandin endoperoxide synthetase.
484 *Science* 196 (1977) 298-300.

- 485 [29] M. Campillos, I. Cases, M.W. Hentze, M. Sanchez, SIREs: searching for iron-
486 responsive elements. *Nucleic Acids Res.* 38 (2010) W360-W367.
- 487 [30] L.A. Kelley, S. Mezulis, C.M. Yates, M.N. Wass, J.E. Sternberg, The Phyre2 web
488 portal for protein modeling, prediction and analysis. *Nat. Protoc.* 10 (2015) 845-
489 858.
- 490 [31] K. Tamura, G. Stecher, D. Peterson, A. Filipski, S. Kumar, MEGA6: Molecular
491 Evolutionary Genetics Analysis version 6.0. *Mol. Biol. Evol.* 30 (2013) 2725-2729.
- 492 [32] N. Saitou, M. Nei, The neiborg-joining method: a new method for reconstructing
493 phylogenetic trees. *Mol. Biol. Evol.* 4 (1987) 406-425.
- 494 [33] F. Silva-Aciare, M. Zapata, J. Tournois, D. Moraga, C. Riquelme, Identification of
495 genes expressed in juvenile *Halotis rufescens* in response to different copper
496 concentrations in the north of Chile under controlled conditions. *Mar. Pollut. Bull.*
497 62 (2011) 2671–2680.
- 498 [34] M.W. Pfaffl, A new mathematical model for relative quantification in real-time
499 RT-PCR. *Nucleic Acids Res.* 29 (2001) 2002-2007.
- 500 [35] J. Bethke, V. Rojas, J. Berendsen, C. Cárdenas, F. Guzmán, J.A. Gallardo, L.
501 Mercado, Development of a new antibody for detecting natural killer enhancing
502 factor (NKEF)-like protein in infected salmonids. *J. Fish Dis.* 35 (2012) 379-388.
- 503 [36] V. Rojas, B. Morales-Lange, F. Guzmán, J.A. Gallardo, L. Mercado,
504 Immunological strategy for detecting the pro-inflammatory cytokine TNF-alpha in
505 salmonids. *Elect J Biotech.* 15(5) (2012) 1-7.
- 506 [37] I. Prieto, S. Hervás-Stubbs, M. García-Granero, C. Berasain, J.I. Riezu-Boj, J.J.
507 Lasarte, P. Sarobe, J. Prieto, F. Borrás-Cuesta, Simple strategy to induce antibodies
508 of distinct specificity: application to the mapping of gp120 and inhibition of HIV-1
509 infectivity. *Eur J Immunol.* 25 (1995) 877-883.
- 510 [38] B. Morales-Lange, J. Bethke, P. Schmitt, L. Mercado, Phenotypical parameters as a
511 tool to evaluate the immunostimulatory effects of beta-laminarin in *Oncorhynchus*
512 *mykiss*. *Aquac Res.* 46 (2015) 2707-2715.

- 513 [39] P. Schmitt, J. Wacyk, B. Morales-Lange, V. Rojas, F. Guzmán, B. Dixon, L.
514 Mercado, Immunomodulatory effect of cathelicidins in response to a beta-glucan in
515 intestinal epithelial cells from rainbow trout. *Dev. Comp. Immunol.* 51 (2015) 160-
516 169.
- 517 [40] G. Snedecor, W. Cochran, *Statistical methods*. 8th ed. (1989) Iowa: Iowa State
518 University Press.
- 519 [41] P.M. Harrison, P. Arosio, The ferritins: molecular properties, iron storage function
520 and cellular regulation. *Biochim. Biophys. Acta* 1275 (1996) 161-203.
- 521 [42] J.P. Durand, F. Goudard, J. Pieri, J.M. Escoubas, N. Schreider, J.P. Cadoret,
522 *Crassostrea gigas* ferritin: cDNA sequence analysis for two heavy chain type
523 subunits and protein purification. *Gene* 338 (2004) 187-195.
- 524 [43] M. De Zoysa, J. Lee, Two ferritin subunits from disk abalone (*Haliotis discus*
525 *discus*): cloning, characterization and expression analysis. *Fish Shellfish Immunol.*
526 23 (2007) 624-635.
- 527 [44] J. Xie, X. Cao, L. Wu, M. Luo, Z. Zhu, Y. Huang, X. Wu, Molecular and
528 functional characterization of ferritin in abalone *Haliotis diversicolor supertexta*.
529 *Acta Oceanol. Sin.* 31 (2012) 87-97.
- 530 [45] J. He, J. Jiang, L. Gu, M. Zhao, R. Wang, L. Ye, T. Yao, J. Wang, Identification
531 and involvement of ferritin in the response to pathogen challenge in the abalone,
532 *Haliotis diversicolor*. *Dev. Comp. Immunol.* 60 (2016) 23-32.
- 533 [46] R.V. Hyne, J.D. Smith, G. Ellender, Tissue and sub-cellular distribution of Fe, Cu,
534 Zn and ^{210}Po in the abalone *Haliotis rubra*. *Mar. Biol.* 112 (1992) 75-8.
- 535 [47] I. Marigómez, M. Soto, M.P. Cajaraville, E. Angulo, L. Giamberini, Cellular and
536 subcellular distribution of metals in mollusks. *Microsc. Res. Tech.* 56 (2002) 358-
537 392.
- 538 [48] T. Roszer, The invertebrate midintestinal gland (“hepatopáncreas”) is an
539 evolutionary forerunner in the integration of immunity and metabolism. *Cell Tissue*
540 *Res.* 358 (2014) 585-695.

- 541 [49] R. Eisler, Compendium of Trace Metals and Marine Biota: Volume 1: Plants and
542 Invertebrates. 1st Edition. Eisler, R. (2010) Elsevier. The Netherlands.
- 543 [50] J.Q. Sheng, Q.C. Shu, J.W. Shi, J.H. Wang, K. Peng, S. Yuan, Y.J. Hong,
544 Immunological function and antibacterial activity of two ferritin proteins from the
545 freshwater pearl mussel *Hyriopsis schlegelii*. Genet. Mol. Res. 15(3) (2016)
546 gmr.15038533.
- 547 [51] L. Wang, F. Yue, X. Song, L. Song, Maternal immune transfer in molluscs. Dev.
548 Comp. Immunol. 48 (2015) 354-359.
- 549 [52] F. Marin, G. Luquet, B. Marie, D. Medakovic, Molluscan shell proteins: primary
550 structure, origin and evolution. Curr. Top. Dev. Biol. 80 (2008) 209-276.
- 551 [53] D.J. Jackson, G. Wörheide, B. Degnan, Dynamic expression of ancient and novel
552 molluscan shell genes during ecological transitions. BMC Evol. Biol. 7 (160)
553 (2007) 1-17.
- 554 [54] N. Hashimoto, Y. Kurita, H. Wada, Developmental role of *dpp* in the gastropod
555 shell plate and co-option of the *dpp* signaling pathway in the evolution of the
556 operculum. Dev. Biol. 366 (2012) 367-373.
- 557 [55] A. Heyland, Z. Vue, C.R. Voolstra, M. Medina, L.L. Moroz, Developmental
558 transcriptome of *Aplysia californica*. J. Exp. Zool. B (Mol. Dev. Evol.) 316 (2011)
559 113-134.
- 560 [56] K.O. Hahn, Nutrition and growth of abalone. In: Hahn, K.O. (Ed.), Handbook of
561 Culture of Abalone and Other Marine Gastropods. CRC Press, Boca Raton, FL,
562 (1989) pp. 135–156.
- 563 [57] K. Brokordt, I. Rojas, C. Cárcamo, R. Rojas, L. Mercado, P. Schmitt,
564 Transcriptional patterns of antimicrobial effectors during early development of the
565 scallop *Argopecten purpuratus* after exposure to the pathogen *Vibrio splendidus*.
566 Proceedings of the Physiomar17 Conference. (2017) Cambridge, UK.
- 567 [58] A. Cozzi, B. Corsi, S. Levi, P. Santambrogio, G. Biasiotto, P. Arosio, Analysis of
568 the biologic functions of H- and L-ferritins in HeLa cells by transfection with

569 siRNAs and cDNAs: evidence for a proliferative role of L-ferritin. *Blood* 103
570 (2004) 2377-2383.

571 [59] S. Li, Identification of iron-loaded ferritin as an essential mitogen for cell
572 proliferation and postembryonic development in *Drosophila*. *Cell Res.* 20 (2010)
573 1148-1157.

574 [60] F. Marin, G. Luquet, B. Marie, D. Medakovic, Molluscan Shell Proteins: Primary
575 Structure, Origin, and Evolution. *Curr Top Dev Biol*, 80 (2008) 209-276.

576 [61] J. Li, L. Li, S. Zhang, J. Li, G. Zhang, Three ferritin subunits involved in immune
577 defense from bay scallop *Argopecten irradians*. *Fish Shellfish Immunol.* 32 (2012)
578 368-372.

579 [62] R. Qiu, Y. Kan, D. Li, Ferritin from the Pacific abalone *Haliotis discus hannai*:
580 analysis of cDNA sequence, expression, and activity. *Fish Shellfish Immunol.* 49
581 (2016) 315-323.

582 [63] S.T. Ong, J.Z. Ho, B. Ho, J.L. Ding, Iron-withholding strategy in innate immunity.
583 *Immunobiol.* 211 (2006) 295-314.

584 [64] M.A. Travers, A.L. Meistertzheim, M. Cardinaud, C.S. Friedman, S. Huchette, D.
585 Moraga, C. Paillard, Gene expression patterns of abalone, *Haliotis tuberculata*, during
586 successive infections by the pathogen *Vibrio harveyi*. *J. Invert. Pathol.* 105 (2010) 289-
587 297.

588

589 **Figure captions**

590 **Figure 1. Nucleotide and deduced amino acid sequences of *Hrfer1* (A) and *Hrfer2***
591 **(B) from *Haliotis rufescens*.** IRE sequence is shaded in yellow. Non-codifying regions
592 are shaded in dark grey. Start codon (ATG) and stop codons are underlined. Asterisk
593 denotes the stop codon in the amino acid sequence. Conserved residues for the
594 ferroxidase site are shaded in green. Conserved residues of the ferrihydrite nucleation
595 centre are shaded in pink. Conserved iron channel residues are shaded in blue. Putative
596 iron-binding regions are shaded in red. Putative N-glycosylation site is shaded in light
597 grey.

598 **Figure 2. Relative basal levels of *Hrfer1* (A) and *Hrfer2* (B) transcripts in different**
599 **tissues of adult *Haliotis rufescens*.** Transcript levels of *Hrfer1* and *Hrfer2* in mantle
600 (Mn), adductor muscle (Mu), gill (Gi), gonad (Go) and digestive gland (Dg) were
601 detected by real-time PCR. β -actin was used as housekeeping gene. All values represent
602 the means \pm S.E. (n = 5 biological replicates). Different letters denote significant
603 differences at $P < 0.05$.

604 **Figure 3. Relative basal levels of *Hrfer1* (A) and *Hrfer2* (B) transcripts in different**
605 **developmental stages of *Haliotis rufescens*.** Assessed developmental stages were
606 gastrula, trochophore, veliger and creeping larva. Metamorphosis stage is indicated by
607 an arrow. β -actin was used as housekeeping gene. All values represent the means \pm S.E.
608 (n = 3 biological replicates). Different letters denote significant differences at $P < 0.05$.

609 **Figure 4. Relative levels of *Hrfer1* and *Hrfer2* mRNA transcript levels in *Haliotis***
610 ***rufescens* after challenge with *Vibrio splendidus*.** Time-course expression analyses of
611 *Hrfer1* and *Hrfer2* transcript levels were measured by RT-qPCR in haemocytes from
612 adult abalone (A and B); and in whole individuals at juvenile stage (C and D). β -actin
613 was used as housekeeping gene. Individuals injected with sterile seawater (SSW), as
614 control, and individuals injected with bacterial suspension are displayed. Values are
615 means \pm S.E. (n = 5 biological replicates per treatment). Different letters denote
616 significant differences at $P < 0.05$.

617 **Figure 5. Ferritin protein levels in juvenile *Haliotis rufescens* challenged with *V.***
618 ***splendidus*.** Ferritin levels were assessed by ELISA in extracts from whole individuals
619 over a period of 48 h post-injection with sterile seawater (SSW), as control; and with
620 bacterial suspension. Values are means \pm S.E. (n = 5 biological replicates per
621 treatment). Different letters denote significant differences at $P < 0.05$.

622

623 Captions of supplementary figures

624 **Figure S1. Production and validation of an anti-ferritin polyclonal antibody for**
625 ***Haliotis rufescens*.** Sequences of the three synthetic peptides (A) used as antigens
626 during the immunization for obtaining antibodies. The best antibodies were obtained
627 against the peptide 1973. The 3D structure (B) of HrFer-1 shows in gold the localization
628 of p1973. (C) Left panel: Immunorecognition of synthetic peptide of ferritin (p1973) by

629 indirect ELISA (calibration curve of anti-HrFer serum against the synthetic peptide used
630 for the immunization; R: Pearson correlation coefficient). Right panel: Determination of
631 antibody specificity by Western blot against mantle protein profile (C: Control group
632 sample; E: challenged group sample).

633 **Figure S2. Multiple sequence alignment of vertebrate and invertebrate ferritin**
634 **subunits.** Conserved residues, important in iron binding and ferroxidation, are
635 contained in boxes. Ferritin sequences shown are from: *Haliotis rufescens* (Hrfer1 and
636 Hrfer2, GenBank: respectively MH006611 and MH006612); *H. discus hannai*
637 (GenBank: ADK60915); *H. diversicolor* (GenBank: AMA34095); *Hyriopsis cumingii*
638 (GenBank: ADZ04889); *Argopecten irradians* ferritin 1 (GenBank: AEN71558);
639 *Rhipicephalus sanguineus* (GenBank: AAQ54715); *Daphnia pulex* heavy (H) chain
640 (GenBank: EFX74776); *Callorhinchus milii* mitochondrial subunit (GenBank:
641 AFM87687); *Danio rerio* middle (M) subunit-like (GenBank: XP_687175); *Homo*
642 *sapiens* heavy (H; GenBank: NP_002023) and light (L; GenBank: NP_000137) ferritin
643 subunits.

644 **Figure S3. Predicted 3D structural models of Hrfer1 (A) and Hrfer2 (B) subunits**
645 **from *Haliotis rufescens*.** The four α helices are coloured in brown, yellow, blue and
646 green. A fifth short helix is coloured in red. Random coils and turns are also displayed.
647 N, N-terminal; C, C-terminal.

648 **Figure S4. Phylogenetic optimal tree of most known nucleotide sequences of**
649 **mollusk ferritin.** Subunits *Hrfer1* and *Hrfer2* references are contained in boxes. The
650 evolutionary history was inferred from the neighbour-joining method. Bootstrap values
651 are shown next to the branches. The tree is drawn to scale, with branch lengths in the
652 same units as those of the evolutionary distances used to infer the phylogenetic tree.
653 GenBank accession numbers are indicated. Ferritins with GenBank accession numbers
654 DQ821493, XM_011440581 and KC754752 (the three sequences at the bottom of the
655 tree) correspond to secretory ferritins. All other sequences correspond to non-secretory
656 ferritins.

657 **Figure S5. Iron responsive element (IRE) analysis of *Hrfer2* and other ferritin**
658 **homologues.** (A) Alignment and sequence comparison with selected ferritin IREs from
659 mollusk ferritin subunits (and the non-molluscan ferritins of *Xenopus laevis* and *Homo*
660 *sapiens*). GenBank Acc No. of each ferritin homologue is indicated. Conserved 5'-

661 CAGTGN-3' loop structure residues and bulged cysteines located five bases upstream
662 are shaded in light grey. The other homologous regions are shaded in dark grey. The
663 percentage similarities of IREs are on the right side. (B) Predicted IRE stem-loop
664 structure of *Hrfer2*, compared with IREs of *Argopecten purpuratus* 2 (GenBank:
665 KT895279), *A. irradians* 2 (GenBank: HQ225741); *Lymnaea stagnalis* (GenBank:
666 X56778) and *Hyriopsis cumingii* 1 (GenBank: HQ896721).

A

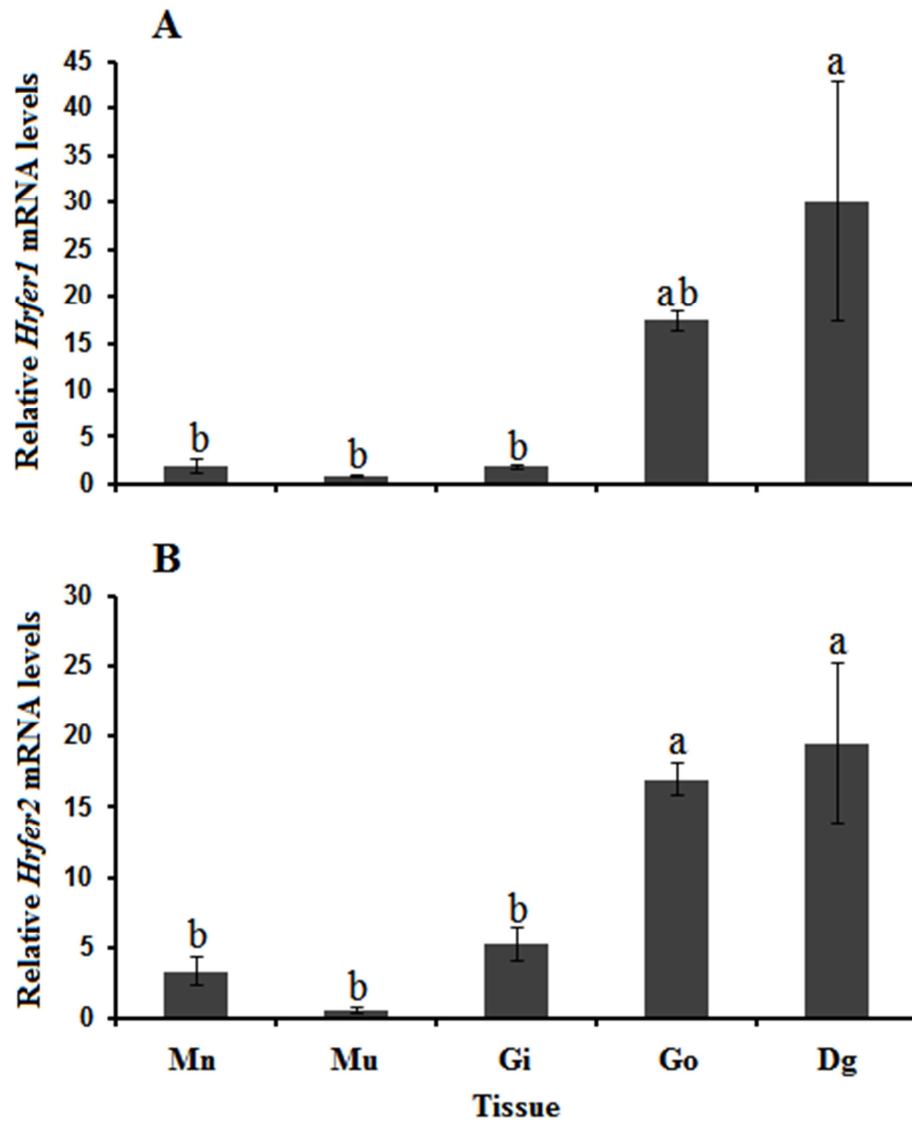
Hrfer1

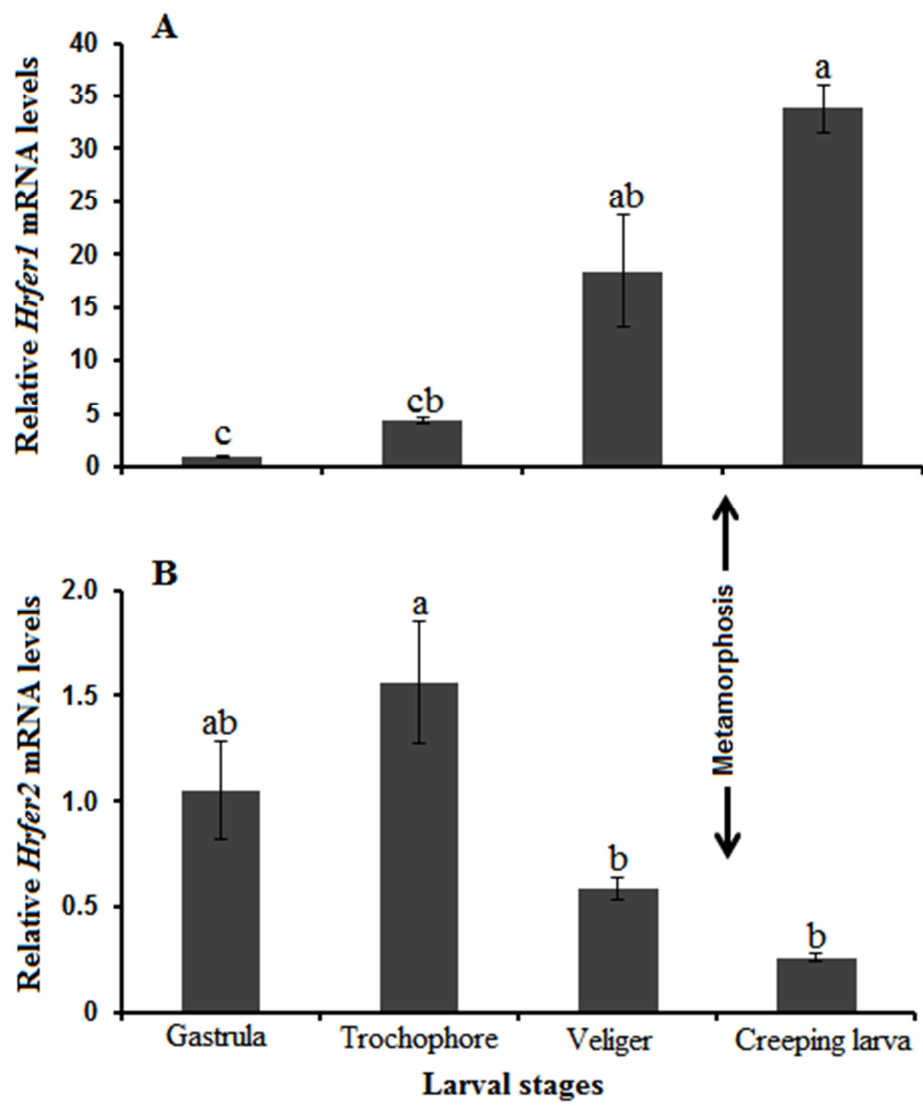
ATGCCAGAAAGTCAAGCAGCTCAGAACTACCACGTCAACAGCGAGGGGGCGTCAACAAACAG
 M P E S Q A R Q N Y H V N S E A G V N K Q
 ATTAACGTCCTGCTGAACTGTAGCTATGTCCTGATTCCATGGCCTGGTATTTGACCGGGAT
 I N V L N C S Y V H S M A W Y F D R D
 GACGTGGCCCTGAAAGGATTTCTTGTAGTTTCTCAAGGATGCCTCTTCCAGGAGCGGAGTTC
 D V A L K G F F E F L K D A S C K K R E E
 GCCGAGAAAATGATGAGTACCAGAACCAGAGAGGTGGGGCATCGTCTGCAGGACATCAAG
 A E K M M K Y Q N Q R G G R I V L Q D I K
 AAGCCGCCCATGACGAATGGGGACAGGCCCTGGACGTGATGCAGTCTGCCCTGGCCCTGAG
 K P P H D E W G T G L D V M Q S A L A L E
 AAGAAGCTCAACCAGGAGTTCCTGGACCTGCACAAAGTGGCGGACTGCAACACTGACCCACAG
 K N V N Q E F L D L H K V A D C N T D P Q
 ATGATGACCTTCTCTGAGGATGAGTTCCTGGAAAGAGGATGCGAGATGATCAAGAACTCTCC
 M M D F L E D E F L E E E V E M I K K L S
 GACCAGTGAACCACTGAAGCGGTTGGACCGGTCGAGAGTACAGTTCGACACAGAG
 D H V T N L K R V G P G L G E Y Q F D H E
 ACTCTCAGTTAAATTGGTCCGGCCCTCCGGTCACCATGGTAACCGATGACAACGCCCGACA
 T L S *
 AGCCTACTGCTTCTGTCTATACTTTCTTGAAGAACTAAAGCCCCCTTCTTGAACCTGGC
 AGCCTGCTTACGTTGACCGGTGACGTGAATTCAAAATGAGATGAAACATTTAATTTTATAC
 GTGCTTATCTTTTATACATTTTGTCTGTTGAATTTGTAAATTTCCCTGTATAAACTCC
 TGTAAAACAACATCTGCAATAAATCCAAGCATGCAAAAAAAAAAAAAAAAAAAAAA

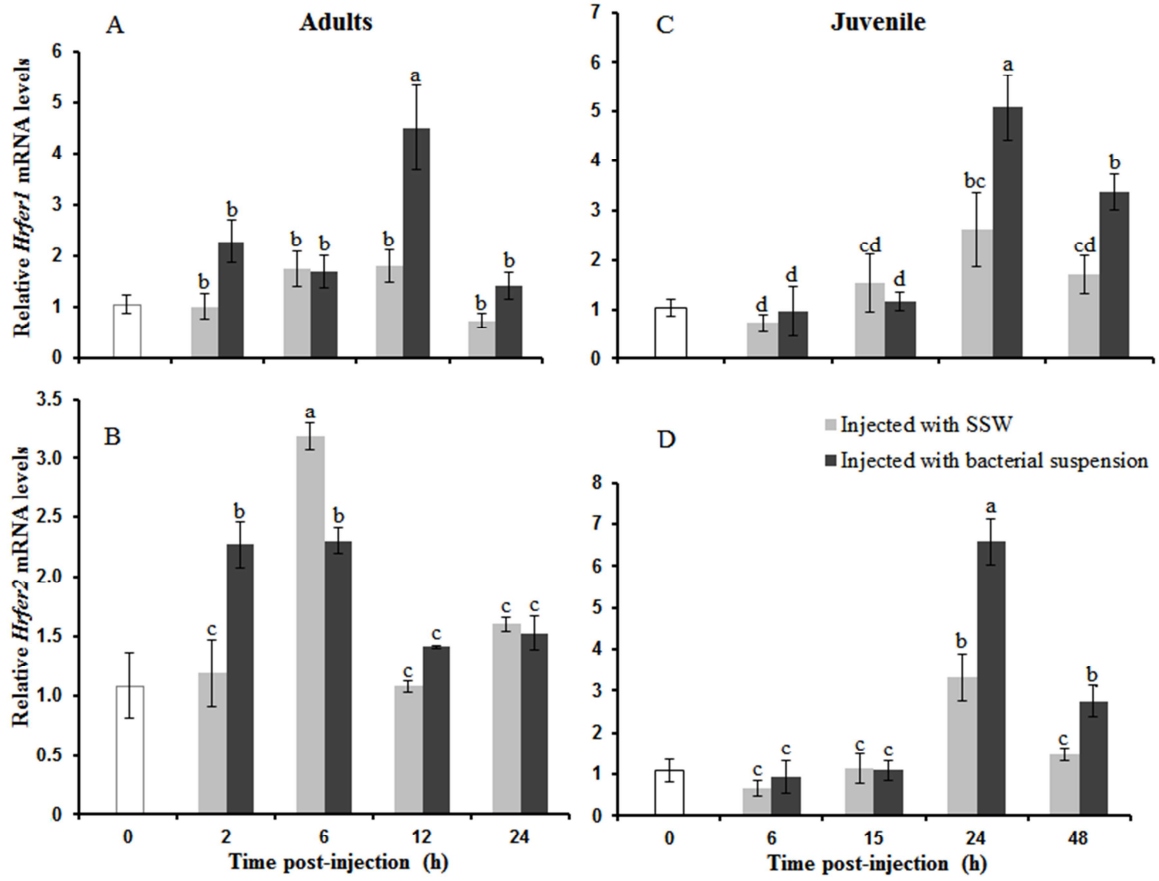
B

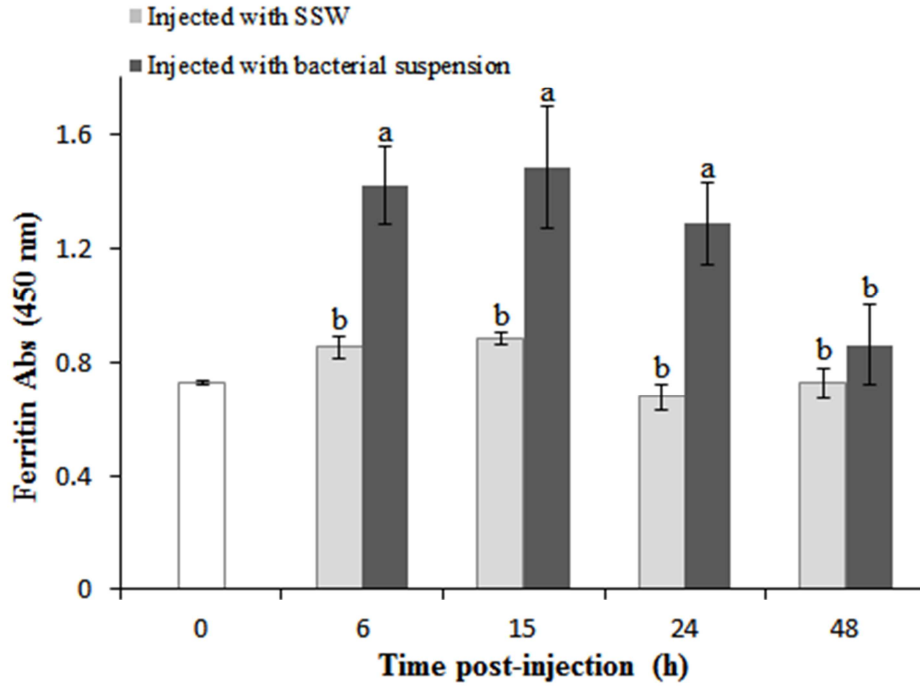
Hrfer2

GACCCTATAGGGCAAGCAGTGGTATCAACCGCAGATACATGGGGAGATGTTTGTCTTGCT
 CGCTCAGTGAACGTACCGGCAAAATCGACGCTATCAAAAGCATTCTTCAACACCCATTTA
 ATCTCATTATTCAGTGTGTCAGTCCGAGAATCTAGCAAGATGGCCAACTCAACCCCG
 M A Q T Q P R
 CCAGAAGTCCACTGCGAGCGAAGCCGGCATCAACCGCCAGATCAATATGACCTGTAC
 Q N F H C E S E A G I N R Q I N M E L Y
 GCCAGCTATACCTACAGTCAATTGGGTTCTACTTCGAGCGCGATGACGTTGCTCTGCCTG
 A S Y T Y Q S I G F Y F E R D D V A L P
 GCTTCAGCAAGTACTTCAAGAGGCATCCGAGGAGCGAGAGCATGCCGAGAAGCTGAT
 G F S K Y F K K A S E E E R E H A E K L M
 GAAGTACCAGAACCCCGAGGAGTCCGATCGTCTGCAGGACATCAAGAAGCCTGACCGG
 K Y Q N T R G G I V L Q D I K K P D R
 GATGAGTGGGGTACAGCACTGGAATCCATGCAGGTGGCTCTGTCCCTGAGAAAGAGTCA
 D E W G T A L E S M Q V A L S L E K N V
 ACCAGTCTTGTGGACCTCCACGCTGTGGCCAGCAACACAGCGACCCACAGATGTGGGA
 N Q S L L D L H A V A S K H S D A Q M C D
 CTTCTGGAGCGAGTACCTTGAGGAGCAGGTGAAGGCCATCAAGGAGATCTCGGACCAC
 F L E S E Y L E E Q V K A I N E I S D H
 ATCACAACCTGAAGCGGTTGGGGCTGGCCTGGGTGAATACATGTAOGACAAGGAGTCCA
 I T N L K R V G A G L G E Y M Y D K E S
 TGGAGTAGTCCCAACCGTCACGTGGGCATAGTCCGACGTGGCCGACCCAGTCAGCCCAT
 M E *
 GTAATGCAATCGTTGATGAACGTTTTGTTCTGTTGAACAGTTTTATATGTTTTGTTGGG
 CTGACATGTGAACATCTGCTTGAATACTGGGGCCGCGAGGCCGTCTTTGATTTCAAT
 CATATTAACCCCAA









Highlights

- Two ferritin sequences were characterized in red abalone, Hrf1 and Hrf2
- Both *ferritins* are present in all tissues and strongly expressed in digestive gland and gonad
- *Hrf1* transcripts increased along with larval development being highest in creeping post-larvae
- Both *ferritins* are upregulated in adults and juveniles challenged with *Vibrio splendidus*
- Ferritin is upregulated at protein level in the juveniles after bacterial challenge